Work function engineering in low-temperature metals

Nicholas D. Orf, Iain D. Baikie, Ofer Shapira, and Yoel Fink

Citation: Appl. Phys. Lett. **94**, 113504 (2009); doi: 10.1063/1.3089677
View online: http://dx.doi.org/10.1063/1.3089677
View Table of Contents: http://apl.aip.org/resource/1/APPLAB/v94/i11
Published by the American Institute of Physics.

Work function engineering in low-temperature metals

Nicholas D. Orf,[1] Iain D. Baikie,[3] Ofer Shapira,[2] and Yoel Fink[1,2,a)]
[1]*Department of Materials Science and Engineering, Massachusetts Institute of Technology, Cambridge, Massachusetts 02139, USA*
[2]*Research Laboratory of Electronics, Massachusetts Institute of Technology, Cambridge, Massachusetts 02139, USA*
[3]*KP Technology Ltd., Wick KW1 5LE, United Kingdom*

(Received 4 December 2008; accepted 6 February 2009; published online 18 March 2009)

Semiconductor devices require conducting electrodes with disparate work functions for their operation. Of recent interest are fluidic processing approaches for large-area devices, which present unique challenges in the identification of materials having disparate work functions but similar melting temperatures. Such materials may be engineered by alloying with low-melting temperature metals. As a demonstration, the work function of tin and four binary tin alloys is measured by ultraviolet photoemission spectroscopy and Kelvin probe method. We demonstrate the control of metal work function by 600 meV through alloying while keeping the melting temperature within a 140 °C range. © *2009 American Institute of Physics*. [DOI: 10.1063/1.3089677]

The variation in work function with alloy composition has important implications in microelectronics where the desire to precisely control device characteristics such as junction barrier height must be balanced by other concerns such as material stability and processability. Although the barrier height in metal-semiconductor contacts can be profoundly influenced by oxides, contamination, and surface states, the work function difference between two materials is often used as a first estimate of the electronic barrier height of two joined materials.[1] For this reason several binary alloy systems have been investigated for their applicability in areas such as field emitters,[2,3] organic light-emitting diode cathodes,[4] and metal gates for field-effect transistors.[5–10] Furthermore, low-temperature processing of metallic electrodes is highly desired since it expands the range of materials that can be incorporated into devices, reduces diffusion and interaction between the metal and semiconductor, and significantly reduces the fabrication cost. Common low-melting temperature solders may be suitable alloys for these reasons and should be considered for metal-semiconductor contacts in any device fabricated with low-temperature, fluid, and high-throughput techniques such as thermal drawing of multimaterial device fibers,[11] as well as inkjet[12] and screen printing.[13] In this paper, the work function of low-melting temperature tin and four binary tin alloys is measured by two techniques in order to determine their potential utility as metal contacts to semiconductor devices

Work function determination is known to depend greatly on both the technique used and surface preparation.[14–16] Using two different methods may reduce the uncertainty due to the different techniques as well as provide important insight into the suitability of the methods for accurate work function determination. Additionally, the fact that all alloys considered in this study contain tin provides a unique twist on typical alloy work function studies where a single binary system is surveyed.[3,5,8–10] These studies, with few exceptions,[17] find that the alloy work function is less than the composition weighted average of the constituent elements. A broad survey over many different systems may give insight into when this trend does and does not hold true.

In addition to elemental tin, alloys studied in this work include $Sn_{91}Zn_9$ ($Sn_{84.8}Zn_{15.2}$ at. %, T_m=199 °C), a mixture of pure element phases; $Sn_{96.5}Ag_{3.5}$ ($Sn_{96.2}Ag_{3.8}$ at. %, T_m =221 °C) and $Sn_{90}Au_{10}$ ($Sn_{93.7}Au_{6.3}$ at. %, T_m=217 °C), mixtures of an intermetallic phase and pure tin; and $Sn_{20}Au_{80}$ ($Sn_{29.3}Au_{70.7}$ at. %, T_m=280 °C), which is a mixture of two intermetallic phases. High purity alloys were obtained in bulk form from the Indium Corporation (Utica, NY) and fashioned into metal coupons before final mechanical polishing under inert atmosphere.

The work function was measured by the scanning Kelvin probe (SKP) technique and ultraviolet photoelectron spectroscopy (UPS). The surface composition was verified by x-ray photoelectron spectroscopy (XPS). SKP was performed with a KP Technology SKP5050 Scanning Kelvin Probe equipped with a 2-mm diameter polycrystalline gold-coated probe head (nominal work function taken to be 5.1 eV).[18] Scans were performed in inert (nitrogen) atmosphere to limit oxidation or gas adsorption that may cause changes in either the sample or probe head work function. The tip-to-sample spacing was held constant (within 1 μm) both during each scan and between samples to minimize stray capacitance errors.[15] Approximately 400 measurements were made over a scanned area of between 6 and 13 mm in each dimension. Measurement uncertainty was taken to be the standard deviation in work function over the entire scanned area. UPS measurements were performed with an Omicron Multiprobe system. Samples were sputter cleaned with an *in situ* argon ion gun immediately prior to measurement. The photon source was a He I (21.2 eV) plasma. Samples were reverse biased to sharpen the onset of secondary electron emission as well as eliminate tertiary electrons from the spectrum. The UV spot size was approximately 1 cm^2. Measurement uncertainty was taken to be the half width of the high kinetic energy Fermi edge cutoff (i.e., zero binding energy). The surface composition as a function of argon ion sputtering time was measured in a separate Kratos Axis Ultra XPS system.

a)Electronic mail: yoel@mit.edu.

TABLE I. Work functions of tin alloys measured by SKP and UPS, work function difference compared to tin, and melting temperature. Estimated error is given in parentheses.

Alloy (wt %)	SKP (eV)		UPS (eV)		$T_{melting}$ (°C)
	Φ	Φ-Φ_{Sn}	Φ	Φ-Φ_{Sn}	
Zn			3.72 (0.19)	−0.42	420
$Sn_{91}Zn_9$	4.17(0.003)	−0.2	3.91 (0.20)	−0.23	199
Sn	4.47(0.008)	0	4.14 (0.19)	0	232
Ag			4.35 (0.12)	0.21	962
$Sn_{96.5}Ag_{3.5}$	4.47(0.008)	0.00	4.12 (0.19)	−0.02	221
Au			5.00 (0.18)	0.86	1064
$Sn_{90}Au_{10}$	4.58(0.016)	0.11	4.28 (0.20)	0.14	217
$Sn_{20}Au_{80}$	4.84(0.014)	0.37	4.59 (0.19)	0.45	280

Alloy work functions measured by the two methods and the UPS-measured work functions of the pure constituent elements are summarized in Table I. The photoemission onset obtained by UPS is given in Fig. 1(b), and representative line scans of the SKP-measured work function can be seen in Fig. 2(b). Two observations may be made immediately. First, the same trend in work function exists with both techniques. The two alloys, Sn and $Sn_{96.5}Ag_{3.5}$, have nearly the same work function. $Sn_{91}Zn_9$ has a notably lower work function, and the gold-tin alloys have the largest work functions of all. Second, there is a systematic offset of 0.25 to 0.33 eV between the techniques with SKP consistently reporting higher work function values. XPS revealed no contamination other than a superficial layer of carbon and oxygen, expected from atmospheric exposure during sample transfer and which disappeared with ion sputtering. Even though differences in sputtering yield between phases could introduce large variations in composition,[19] the surface composition after sputtering was found to be Sn_{100}, $Sn_{93.5}Zn_{6.5}$, $Sn_{97.2}Ag_{2.8}$, $Sn_{88.3}Au_{11.7}$, and $Sn_{11.7}Au_{88.3}$, close to the bulk values.

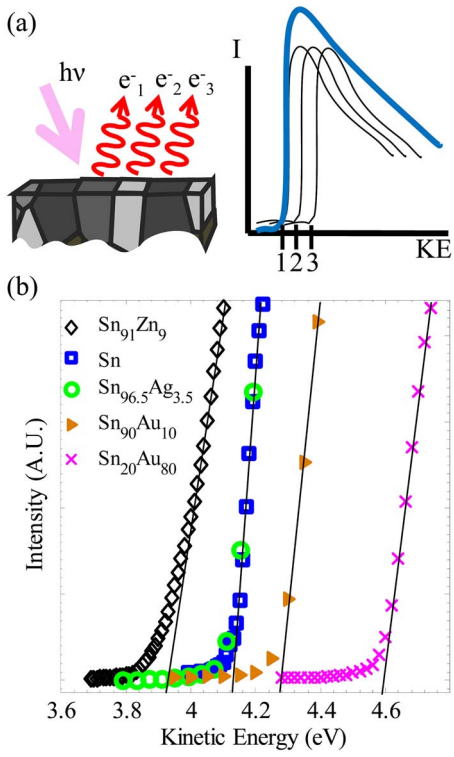

FIG. 1. (Color online) Onset of photoemission for alloys. (a) Schematic diagram of the photoemission process from the polycrystalline metal. Distribution of emitted electrons is the convolution (blue line) of emission spectra from individual surface patches (regions 1–3). The material work function is observed to be equal to the energy of the lowest-energy electron emitted from the surface. (b) Experimental data. UPS work function is determined by extrapolation of the indicated solid line to the kinetic energy axis.

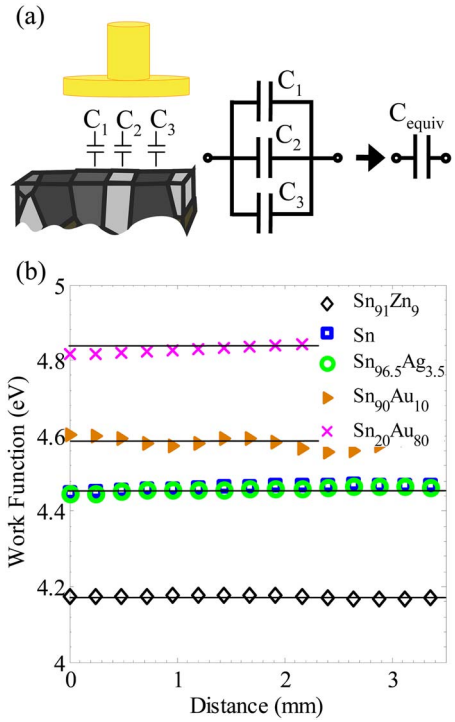

FIG. 2. (Color online) Work function of alloys by SKP. (a) Schematic diagram of the Kelvin technique. The measured capacitance (proportional to the probe and sample work function difference) is an area-weighted average of the individual patch contact potential differences. (b) Experimental data. Solid lines are drawn as guides to the eye.

Errors may originate from the experimental procedure. The KP method is very precise but measures only the difference in work function between the sample and the tip. Thus unaccounted for deviations in the probe head work function would introduce a constant shift in the measured work function value. Although samples were kept under inert atmosphere during cleaning and the KP measurement, adsorption of even inert gases may cause shifts in the sample and probe work functions. Indeed, the work function of gold has been observed to shift up to 0.4 eV under different atmospheres.[20] Additionally, argon sputtering has also been shown to cause shifts in work function due to preferential sputtering, surface roughening, or both.[15,19,21,22] Finally, although extreme care was taken to generate and maintain clean sample surfaces in both sets of experiments, the possibility of surface oxidation cannot be ruled out. XPS measurements do suggest that sputter-induced surface segregation or preferential sputtering is minimal for the alloys considered here.

A difference in the work function determined by these two methods is, in fact, expected. The work function of the different crystal facets is known to differ; the magnitude of which has been extensively studied.[23–25] This anisotropy is closely related to the packing density of the facet, with the closest-packed planes generally exhibiting larger work functions than lower-density planes. Because the surface of a

polycrystalline material is a collection of randomly oriented crystallites, surface patches corresponding to different grains are expected to have different work functions. The addition of entirely separate crystalline phases, as is the case with eutectic alloys, introduces even more facets and work function patches on the sample surface. The work function anisotropy in crystal facets has been numerically predicted and experimentally observed to range from approximately 100–800 meV, depending on the element and crystal facet.[25,26] In light of the samples' polycrystalline nature, the two techniques used in this study will report different work function values. The KP method essentially measures the capacitance per area. Thus the SKP-determined work function is an area-weighted average of all work function patches underneath the probe head [Fig. 2(a)]. However, photoemission spectroscopy is most sensitive to the lowest work function patch, as the lowest kinetic energy electrons originate from this area [Fig. 1(a)].[14] Our results are consistent with the idea that UPS measurements should yield a lower work function than SKP, and this difference has been observed previously in other systems (for example, in indium tin oxide).[16] The magnitude of the difference between the lowest and average work function values is hard to predict for the systems presently considered because the magnitude of the anisotropy of the crystalline facets considered in this work is not known. However, a shift of a few hundred meV seems reasonable, considering that most metals exhibit anisotropy in this range.

In order to gain better insight into the work function trends, the work function of the component elements was measured with UPS. They were found to be 3.72, 4.14, 4.35, and 5.0 eV for zinc, tin, silver, and gold, respectively, consistent with the literature.[18,27] Most alloys have a measured work function less than that of the weighted average of the two component elements, consistent with the general trend observed in other studies.[3,5,8–10,28,29] For example, the work function of zinc measured by UPS is 3.7 eV, and a simple mixing rule would predict the work function of $Sn_{91}Zn_9$ to be 4.11 eV, nearly 150 meV higher than what was actually measured. A unique situation exists in the gold-tin alloy system. While the work function of the gold-rich alloy measured by UPS is indeed ~200 meV less than what the mixing rule would predict, the tin-rich alloy (a composite of pure tin and $AuSn_4$) work function of 4.58 eV is ~100 meV greater than the value predicted by the components' weighted average work function. The same conclusion is reached when taking the weighted average of the KP-derived gold and tin work functions (5.1 and 4.47 eV, respectively). We note that Li *et al.*[17] found several intermetallic compounds having work functions notably larger than their composition-weighted average.

In conclusion, the work function of tin and four tin-based eutectic alloys has been measured by two different methods. The results between the two methods agree, although there is a constant offset of about 0.3 eV, most likely due to the inherent differences in technique. Error may also be due to poor surface quality, e.g., incomplete or preferential ion sputtering, surface roughening, or gas adsorption. The work function of the four alloys were found to range from 3.92 to 4.59 eV and 4.18 to 4.84 eV as measured by UPS and SKP, respectively. Furthermore, with the exception of $Sn_{90}Au_{10}$, the alloy work functions are found to be less than the composition weighted average of constituent elements, an observation consistent with previous studies. Thus the work function of metal contacts in low-temperature or fluid-processed electronic devices may be tuned for a specific purpose, suggesting that important electronic properties such as the built-in voltage for diodes or threshold voltage for transistors, may be controlled by the proper selection of electrode material.

We wish to thank M. Baldo for the generous use of UPS system, V. Wood and A. Abouraddy for critical reading of the manuscript, and E.L. Shaw and D. Lange for their help with the XPS measurements. N.O. gratefully acknowledges support from the National Defense Science and Engineering Graduate Program. This research was supported in part by the U.S. Army Research Office through the Institute for Soldier Nanotechnologies at MIT (Contract No. W911NF-07-D-0004) as well as by the MRSEC Program of the National Science Foundation (Grant No. DMR – 0819762).

[1] S. Sze and K. Ng, *Physics of Semiconductor Devices*, 3rd ed. (Wiley, New York, 2006).
[2] O. Auciello, J. C. Tucek, A. R. Krauss, D. M. Gruen, N. Moldovan, and D. C. Mancini, J. Vac. Sci. Technol. B **19**, 877 (2001).
[3] R. E. Thomas and J. W. Gibson, Appl. Surf. Sci. **29**, 49 (1987).
[4] H. Suzuki, Appl. Phys. Lett. **69**, 1611 (1996).
[5] B.-Y. Tsui and C.-F. Huang, IEEE Electron Device Lett. **24**, 153 (2003).
[6] I. Polishchuk, P. Ranade, T. S. King, and C. Hu, IEEE Electron Device Lett. **23**, 200 (2002).
[7] T. Matsukawa, Y. X. Liu, M. Masahara, K. Ishii, K. Endo, H. Yamauchi, E. Sugimata, H. Takashima, T. Higashino, E. Suzuki, and S. Kanemaru, Microelectron. Eng. **80**, 284 (2005).
[8] B. Chen, N. Biswas, and V. Misra, J. Electrochem. Soc. **153**, G417 (2006).
[9] H. Zhong, S. N. Hong, Y. S. Suh, H. Lazar, G. Heuss, and V. Misra, Tech. Dig. - Int. Electron Devices Meet. **2001**, 20.25.21.
[10] R. M. Todi, M. S. Erickson, K. B. Sundaram, K. Barmak, and K. R. Coffey, IEEE Trans. Electron Devices **54**, 807 (2007).
[11] A. F. Abouraddy, M. Bayindir, G. Benoit, S. D. Hart, K. Kuriki, N. D. Orf, O. Shapira, F. Sorin, B. Temelkuran, and Y. Fink, Nat. Mat. **6**, 336 (2007).
[12] C. N. Hoth, S. A. Choulis, P. Schilinsky, and C. J. Brabec, Adv. Mater. **19**, 3973 (2007).
[13] S. E. Shaheen, R. Radspinner, N. Peyghambarian, and G. E. Jabbour, Appl. Phys. Lett. **79**, 2996 (2001).
[14] L. Ley and M. Cardona, *Photoemission in Solids I* (Springer, New York, 1978).
[15] I. D. Baikie, K. O. Vanderwerf, H. Oerbekke, J. Broeze, and A. Vansilfhout, Rev. Sci. Instrum. **60**, 930 (1989).
[16] J. S. Kim, B. Lagel, E. Moons, N. Johansson, I. D. Baikie, W. R. Salaneck, R. H. Friend, and F. Cacialli, Synth. Met. **111**, 311 (2000).
[17] W. Li, Y. Wang, M. Cai, and C. W. Wang, J. Appl. Phys. **98**, 083503 (2005).
[18] D. R. Lide, *CRC Handbook of Chemistry and Physics* (CRC, New York, 2008).
[19] M. P. Seah, C. A. Clifford, F. M. Green, and I. S. Gilmore, Surf. Interface Anal. **37**, 444 (2005).
[20] W. N. Hansen and K. B. Johnson, Surf. Sci. **316**, 373 (1994).
[21] N. Matsunami, Y. Yamamura, Y. Itikawa, N. Itoh, Y. Kazumata, S. Miyagawa, K. Morita, R. Shimizu, and H. Tawara, At. Data Nucl. Data Tables **31**, 1 (1984).
[22] Y. Yamamura and H. Tawara, At. Data Nucl. Data Tables **62**, 149 (1996).
[23] R. Smoluchowski, Phys. Rev. **60**, 661 (1941).
[24] C. J. Fall, N. Binggeli, and A. Baldereschi, Phys. Rev. B **61**, 8489 (2000).
[25] H. L. Skriver and N. M. Rosengaard, Phys. Rev. B **46**, 7157 (1992).
[26] C. J. Fall, N. Binggeli, and A. Baldereschi, Phys. Rev. B **65**, 045401 (2002).
[27] B. B. Alchagirov, O. I. Kurshev, T. M. Taova, and K. B. Khokonov, Tech. Phys. **51**, 1624 (2006).
[28] C. D. Gelatt and H. Ehrenreich, Phys. Rev. B **10**, 398 (1974).
[29] S. C. Fain and J. M. McDavid, Phys. Rev. B **9**, 5099 (1974).